Supplementary

1-Deposition curves

We are able to provide deposition curves, i.e., the number of successive particles captured, singles or aggregates, against the number of particles that pass through the pore (Fig. 1) by counting each deposition event within the pore and determining the features of the deposited objects and also the number of particles that flow through the pore between each deposition event.

Clearly the shapes of the deposition curves are not the same. However, most of the time single particles are first captured by the pore wall even though very few aggregates can also deposit. During the clog formation, the rate of particles passing through the pore is not constant and there are moments where a considerable number of particles passes through the pore between two deposition events, while for other moments this number is much smaller and thus the clog formation is more "continuous". This rate of deposition is directly linked to degree of local fouling of the pore cross section and also to the type of object that deposit.

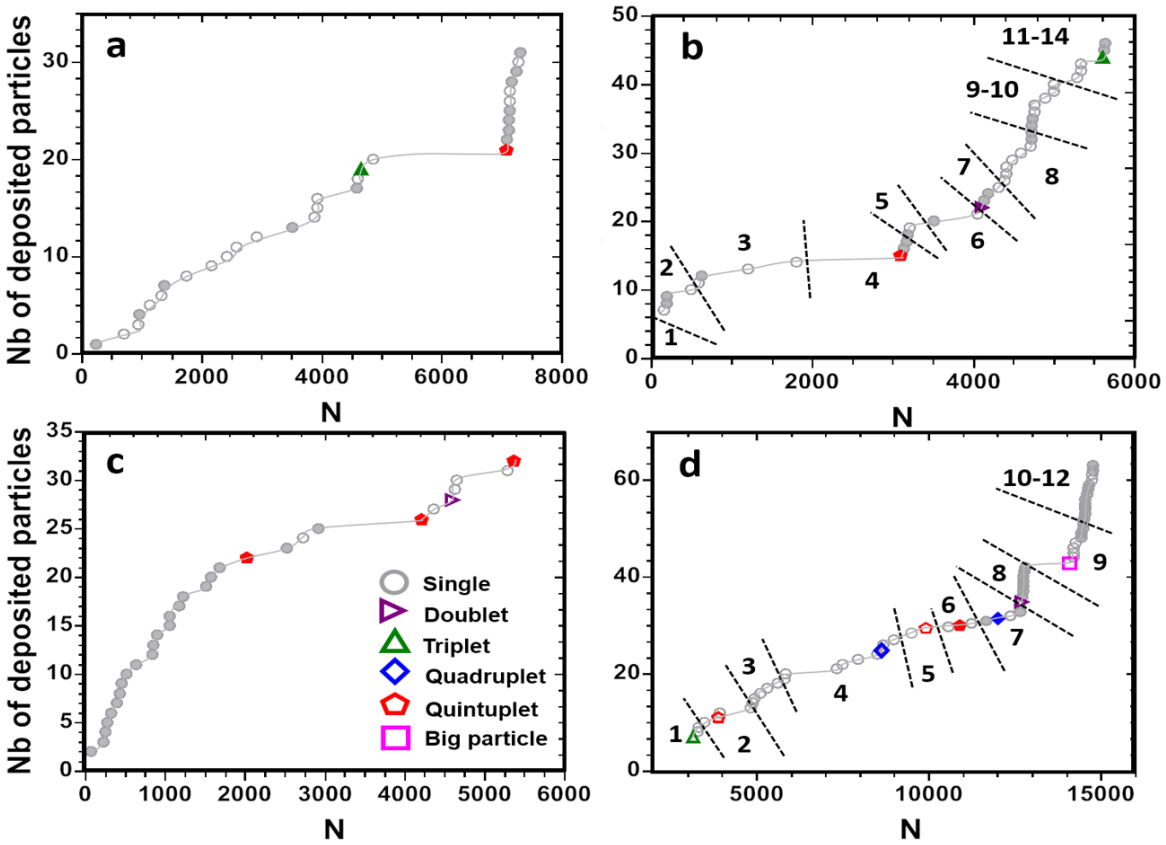

Fig. 1: Deposition curves for the 1st (a-b) and the 2nd clog scenario (c-d). The full symbols correspond to the objects that contribute to the clog since they are captured exactly where the clog eventually blocks the pore, while the open symbols are the objects that do not contribute directly to the clog, their deposition taking place elsewhere within the pore, where the growth of the deposit on the pore walls remains limited. The term "large aggregate" in the legend corresponds to aggregates composed of 6 particles or more. The images of the clog formation corresponding to the plots b and d are shown in figure 4 and 5, respectively. Each image number in these figures are related to the different zones of the deposition curves labelled by a number and delimited by oblique dashed lines. The continuous line on each plot are guides to the eyes.

In the 1st plot, (a), few single particles are captured when a triplet deposits. This aggregate helps capture a larger ones whose deposition reduces the local pore cross section significantly enough to allow the capture of single particles up to the complete pore blocking. We observe a similar succession of deposition events in 3rd plot, (c), in which there is much deposition of single particles prior the capture of the first aggregate, a quintuplet. In this case the pore is completely block by another quintuplet rather by the successive deposition of single particles. Consecutive images in figures 4 and 5 in the main text help understand the deposition curves in the plots b and d respectively.

2-Evolution of the repartition between the two clogging categories with the flow conditions

We determine how the separation between the two clogging categories depends on the flow conditions for PMMA particles. We have seen that there are two clogging regimes when we look at the evolution of N^* with Q. In the 1st clogging regime, $0.008 < Q < 1$µl/min, N^* is constant and roughly equal to 2000 particles, a value high enough to observe several aggregates flowing through the pore according to the particle size distribution (Fig. 2, top). In this first clogging regime clogs mainly belong to the first category (sup. Fig. 2, top-left). For $Q<0.15$µl/min the average number of deposited aggregates is constant, irrespective the aggregate size (sup Fig. 3a) and for $0.15<Q<1$µl/min the number of objects, larger than triplets, slightly increases while that of the smaller ones falls. In this later Q range, the detachment by the flow of doublets and triplets increases with Q while it does not affect larger aggregates (sup Fig. 3c). This means that the average size of the deposited aggregates increases with Q (sup Fig 3d). Note that there is often detachment of single particles from the pore wall in this first regime, more particularly at the end of the clogging process, where the remaining cross section of the pore is small and thus the local shear rate is high, which favors particle detachment (sup Fig. 3b and f).

In the 2nd regime, for $Q > 1$µl/min, there is first a fivefold increase of N^* followed by a smoother increase of N* with Q (Fig. 3a, top left). Almost all the clogged pores belong to the second category. The consecutive deposition of large aggregates involves less capture of smaller objects, from single up to triplet (sup Fig. 3a). It is worth mentioning that there is lower capture probability for all types of aggregate, still due to flow erosion. In addition to the lower capture probability, the number of detachment events of single particles or of part of the deposit increases with Q (sup Fig. 3f). Even if large aggregates have more contact points with the deposit the local shear rate is sufficient to detach them from $Q > 1$µl/min.

Finally, we note that the clog formation is rather irreversible for both regimes since there is only few percent of de-clogging events (sup Fig. 3e). Moreover, the structure of the deposit that accumulates on the pore walls does not evolve over time significantly since we observed local particle/aggregate rearrangements only for 15 to 20% of the clogs as they built-up (sup Fig. 3e). All together these results suggest that the main difference between the two clogging regimes is the influence of the erosion at higher flow rates which prevent the deposition of single particles and doublets-triplets and also to a lesser extent of larger aggregates. This erosion thus leads to an increase of N^* in the 2nd regime since the clogging process mainly relies on large aggregates that are less numerous. Indeed, to block the pore in this regime few large aggregates are needed which is confirmed by the increase of the aggregate dimension and also the number of particle per aggregate with Q (sup Fig. 3d and g).

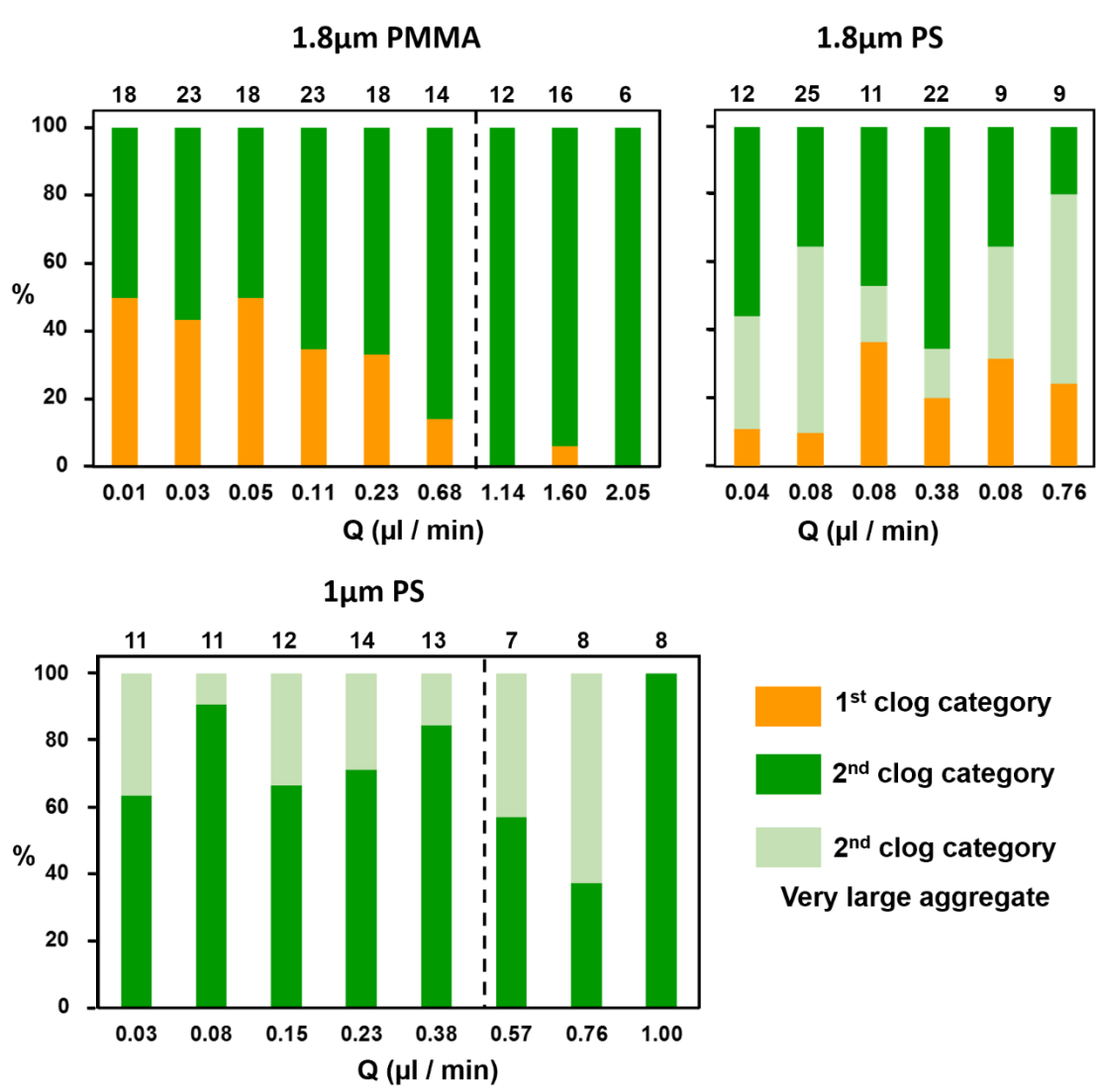

Fig. 2: Repartition of the clog experiments between the two categories for the 1µm PS (bottom), 1.8µm PMMA and PS particles (top) in the different flow conditions. The number of trials for each flow rate value is indicated at the top of the graphs. For 1µm and 1.8µm PS particles we make the distinction inside the 2nd category between the aggregates with L_{max} > W and the very large aggregates that are sieved at the pore entrance.

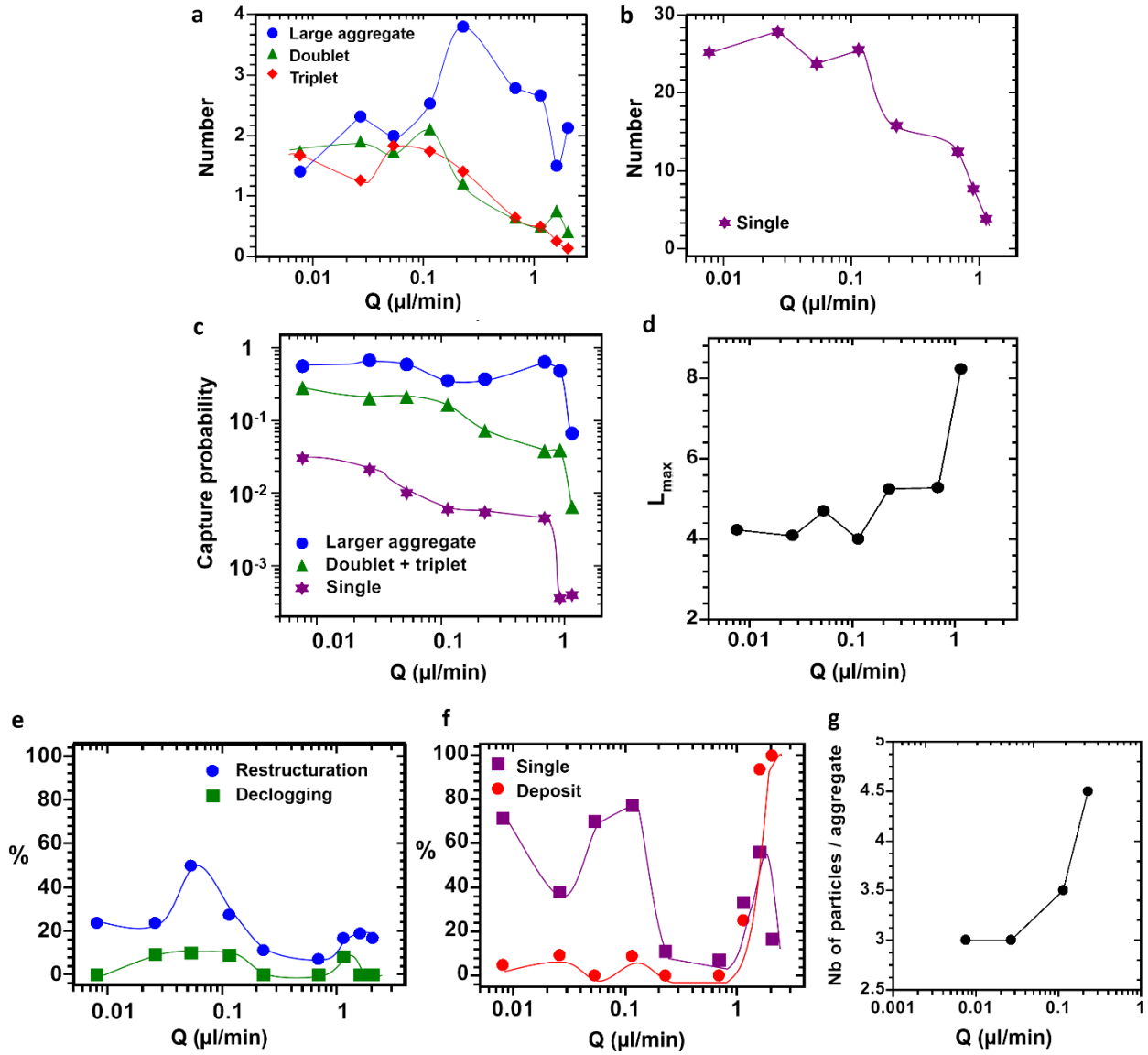

Fig. 3: (a) Average number of aggregates of the different types with different sizes that deposit in the pore during one experiment. (b) Average number of single PMMA particles that deposit in the 1st 20µm of the pore during one experiment. (c) Capture probability of the different types of PMMA particles of the suspension with the flow rate. (d) Variation of L_{max} with Q. (e) Percentage of experiments in which there is a detachment event of a single particle or of a part of the deposit. (f) Percentage of experiments in which there is a restructuration/rearrangement inside the deposit or a de-clogging of the pore. (g) Variation of the average number of particles per aggregate with Q. All the continuous lines on the plots are guides to the eyes.

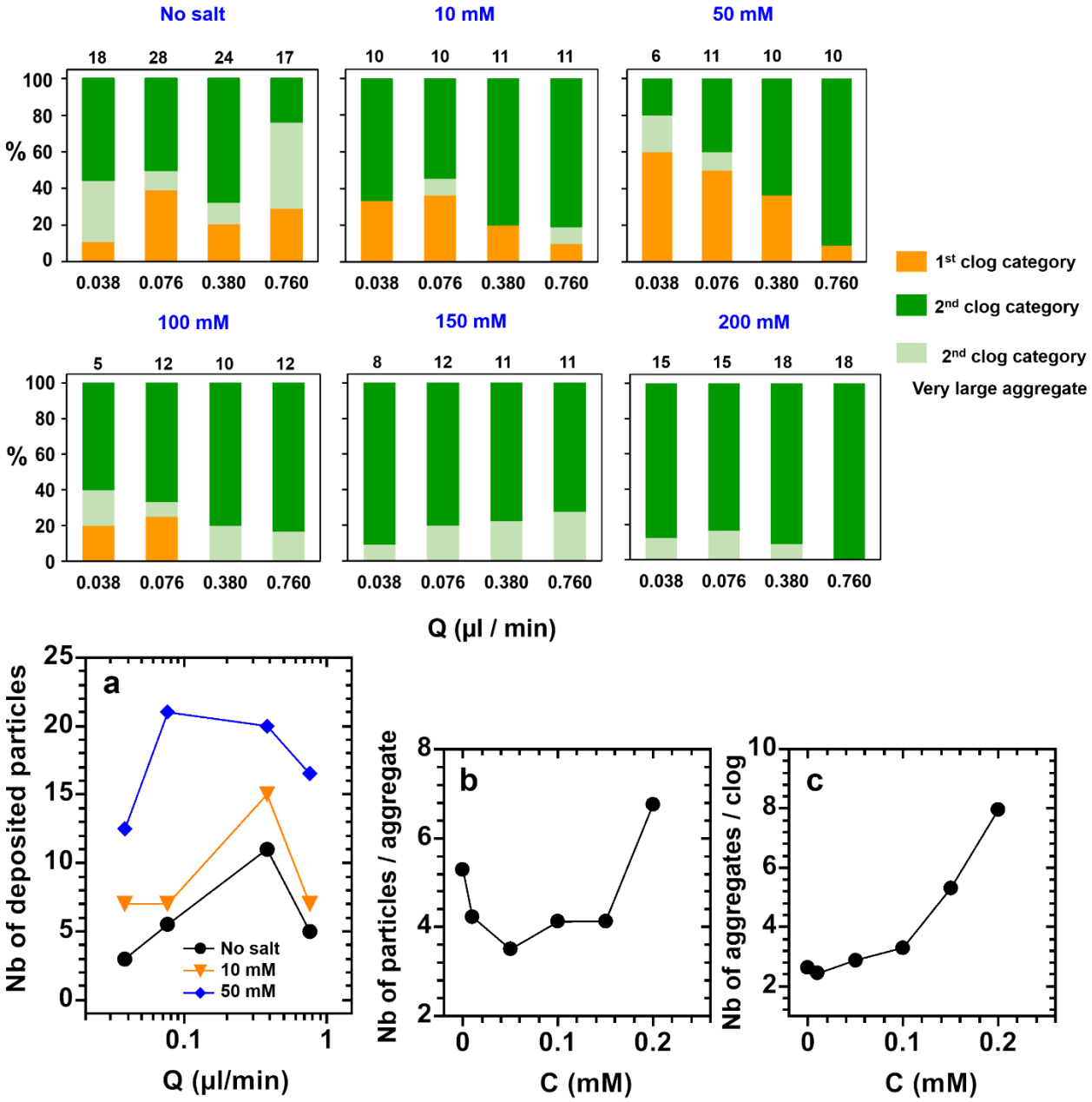

Fig. 4: (Top) Comparisons between the clog experiments for the two clog categories for the 1.8µm PS dispersed in solutions with various amount of NaCl salt. The number of trials for each flow rate value is indicated at the top of the graphs. With no salt added most of the clog belong to the second category (top left), with more than 70% of the clogs. For *C*=10mM, even though the surface charges of the pore walls are not completely screened, the particle deposition is enhanced compared to the salt free case (a), favoring the formation of clog of the 1st category, (top middle). This trend is inversed when the flow rate increases and the 2nd clog category becomes the dominant one. This is due to the lower probability of deposition for the smaller aggregates, with these being more easily wiped off by the flow. A similar decrease of the population of the 1st clog category with *Q* is observed for *C*=50mM, concentration for which the surface charge of the PDMS is totally screened (top right). However, for this salt concentration the second clog category remains dominant for the overall range of *Q*. The 1st clog category becomes even more restricted to the lower flow rates for *C*=100mM (bottom left). The decrease of the number of clogs of the first category with *Q* is mainly due to the erosion of the smaller aggregates by the flow while the larger ones are less eroded (a). Closer to the CCC of the suspension from *C*=150mM, clogs belong to the 2nd category (bottom middle and right), indicating that there are always large aggregates within the clogs. The number of clogs that involve aggregates larger the pore width, also increases with the salt concentration. From *C*=100mM up to 200mM, around 20% of the clogs are mainly composed of one of these large objects, whatever the flow rate (b). (Bottom) (a) Average Number of single particles deposited in a pore for suspensions of 1.8µm PS particles with various amount of NaCl salt. (b) Average number of particles inside the aggregates that form the clogs with the salt concentration *C*. (c) Average number of aggregates inside a clog vs. *C*.

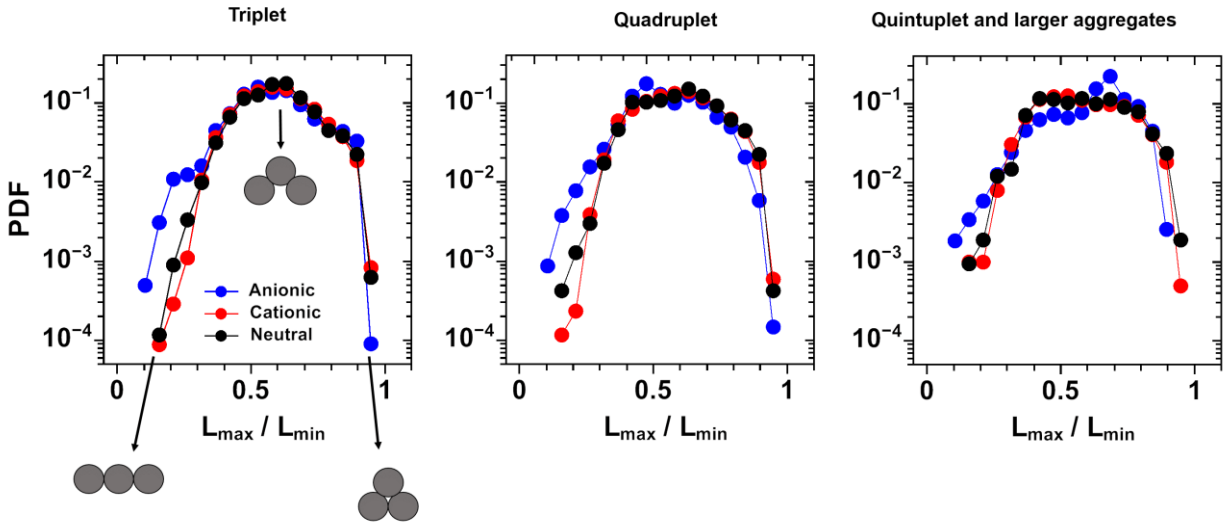

Fig. 5: Probability density functions of the aspect ratio L_{max}/L_{min} for triplet (left), quadruplet (middle) and quintuplet and larger aggregates (right) for the different PS coated dispersions. Shapes of triplet corresponding to various aspect ratios (left). The median value of the aspect ratio is equal to 0.6, irrespective of the aggregate and suspension type.